Journal of Volcanology and Geothermal Research 301 (2015) 107–115

Contents lists available at ScienceDirect

Journal of Volcanology and Geothermal Research

journal homepage: www.elsevier.com/locate/jvolgeores

Maximum horizontal range of volcanic ballistic projectiles ejected during explosive eruptions at Santorini caldera

K.I. Konstantinou *

Dept of Earth Sciences, National Central University, Jhongli, 320, Taiwan

ARTICLE INFO

Article history:
Received 12 February 2015
Accepted 16 May 2015
Available online 27 May 2015

Keywords:
Santorini
Ballistic projectiles
Volcanic hazard
Aegean

ABSTRACT

This study investigates the hazard posed by Volcanic Ballistic Projectiles (VBPs) to the Santorini islands considering eruption scenarios that include low (VEI = 2–3) and higher energy (VEI >3) eruptions. A model that describes rapid decompression of pressurized magma below a caprock along with its fragmentation and acceleration of particles is utilized for estimating initial velocities during vulcanian-style eruptions. These initial velocities are inserted into the ballistic equations assuming that VBPs have a cube-like shape, are subjected to gravity/drag forces and are launched into a zone of reduced drag. Four different diameters of VBPs are considered (0.35 m, 1.0 m, 2.0 m, 3.0 m) and also different values of gas fractions and extent of the reduced drag zone are investigated. The results of these calculations show that an area of 1–2 km width along the western coast of Thera will be within the maximum range of VBPs, provided that the eruptive vent will develop either on Nea Kameni or between Nea Kameni and Thera. Initial velocities for higher energy eruptions are estimated by considering the conversion efficiency of thermal to kinetic energy. For the case of an eruption with VEI = 4 and a number of vents centered between Nea and Palea Kameni, calculations show that the coastal areas of Thera and Therasia are within the maximum horizontal range of VBPs with diameter larger than 0.35 m. As the exact position of the eruptive vent seems to be of crucial importance for determining the areas at risk, continuous seismic and geodetic monitoring of the caldera is needed in order to decipher its likely location.

1. Introduction

Volcanic Ballistic Projectiles (hereafter called VBPs) can be defined as particles above a certain diameter (>0.1 m) of any origin that tend to separate rapidly from the eruptive column, following nearly parabolic trajectories before they impact the Earth's surface (Alatorre-Ibargüengoitia et al., 2012). VBPs represent a significant volcanic hazard that can potentially cause damage to man-made structures and serious injury to the inhabitants of the area around the eruption site. These hazardous effects stem from two properties that VBPs have, namely their high impact energy and elevated temperature. The former property accounts for the fact that large projectiles are capable of penetrating building materials such as cement and the latter one is responsible for triggering fires should VBPs fall within a vegetated area. Observations from volcanoes worldwide suggest that VBPs attain ejection velocities in the range of 50–600 m/s, they have diameters of few centimeters to several meters and their maximum horizontal range may vary from hundreds of meters to several kilometers (Nairn and Self, 1978; Yamagishi and Feebrey, 1994; Kilgour et al., 2010; Harris et al., 2012; Maeno et al., 2013). In an effort to mitigate the risks posed by VBPs, volcanologists have taken advantage of the rather predictable trajectories that VBPs follow and have tried to delineate their impact locations. Such calculations take into account that VBPs are subjected to gravity and drag forces and that their trajectories depend on the initial conditions at the time when they were ejected from the eruption vent (Walker et al., 1971; Wilson, 1972; Fagents and Wilson, 1993; Bower and Woods, 1996).

Volcanism in the southern Aegean is the consequence of the subduction of the African slab beneath the Eurasian plate which results in the formation of a well-developed volcanic arc (Vougioukalakis and Fytikas, 2005). Santorini caldera is a very active volcanic center of this arc, having produced numerous explosive eruptions over the last 250 ka, the most famous of these being the Late Bronze Age (ca. 1613 BC, VEI = 7) Minoan eruption (Bond and Sparks, 1976; Heiken and McCoy, 1984; Druitt and Francaviglia, 1992; Vougioukalakis and Fytikas, 2005; Friedrich, 2013). Subsequently, several smaller eruptions with VEI between 2 and 3 occurred in the time period from 197 BC to 1950 AD, and the small islands of Palea and Nea Kameni that lie in the center of the caldera were created by this activity. For the last 60 years, the volcanic system had been relatively quiet with only minor hydrothermal and seismic activity (Dimitriadis et al., 2009). However, this situation changed in 2011 when significant uplift and increased seismicity rates were detected within the caldera (Newman et al., 2012; Parks et al., 2012; Foumelis et al., 2013; Konstantinou et al., 2013; Lagios et al., 2013; Papoutsis et al., 2013). Even though

* Fax: +886 3 4222044.
E-mail address: kkonst@cc.ncu.edu.tw.

http://dx.doi.org/10.1016/j.jvolgeores.2015.05.012
0377-0273/

this unrest did not culminate into an eruption, it did put forward the issue of the volcanic hazards posed by future eruptive activity and how authorities should plan to cope with them. Vougioukalakis and Fytikas (2005) have published a zonation map (Fig. 1) for different volcanic hazards that are expected to affect the Santorini island complex and especially Thera island, whose population is greatly increased by a large influx of tourists every summer. The delineation of the hazard area due to VBPs impact is mostly based on observations of the effects from previous eruptions (even though the authors do not refer explicitly to these observations) and implies that the most populated areas on Thera are out of VBPs range.

This work aims at estimating the maximum horizontal range of VBPs at Santorini caldera for different eruption scenarios that range from small eruptions with Volcanic Explosivity Index (Newhall and Self, 1982) (hereafter called VEI) between 2 and 3, as well as larger ones (VEI > 3). First, a caprock model proposed by Alatorre-Ibargüengoitia et al. (2010) approximating conditions during small volume explosive eruptions is used in order to estimate initial velocities of ejected VBPs. Initial velocities for higher energy eruptions are calculated by using an approach based on the conversion efficiency of thermal to kinetic energy (Sato and Taniguchi, 1997). The calculated ejection velocities are then coupled to a ballistic model that describes the trajectories of

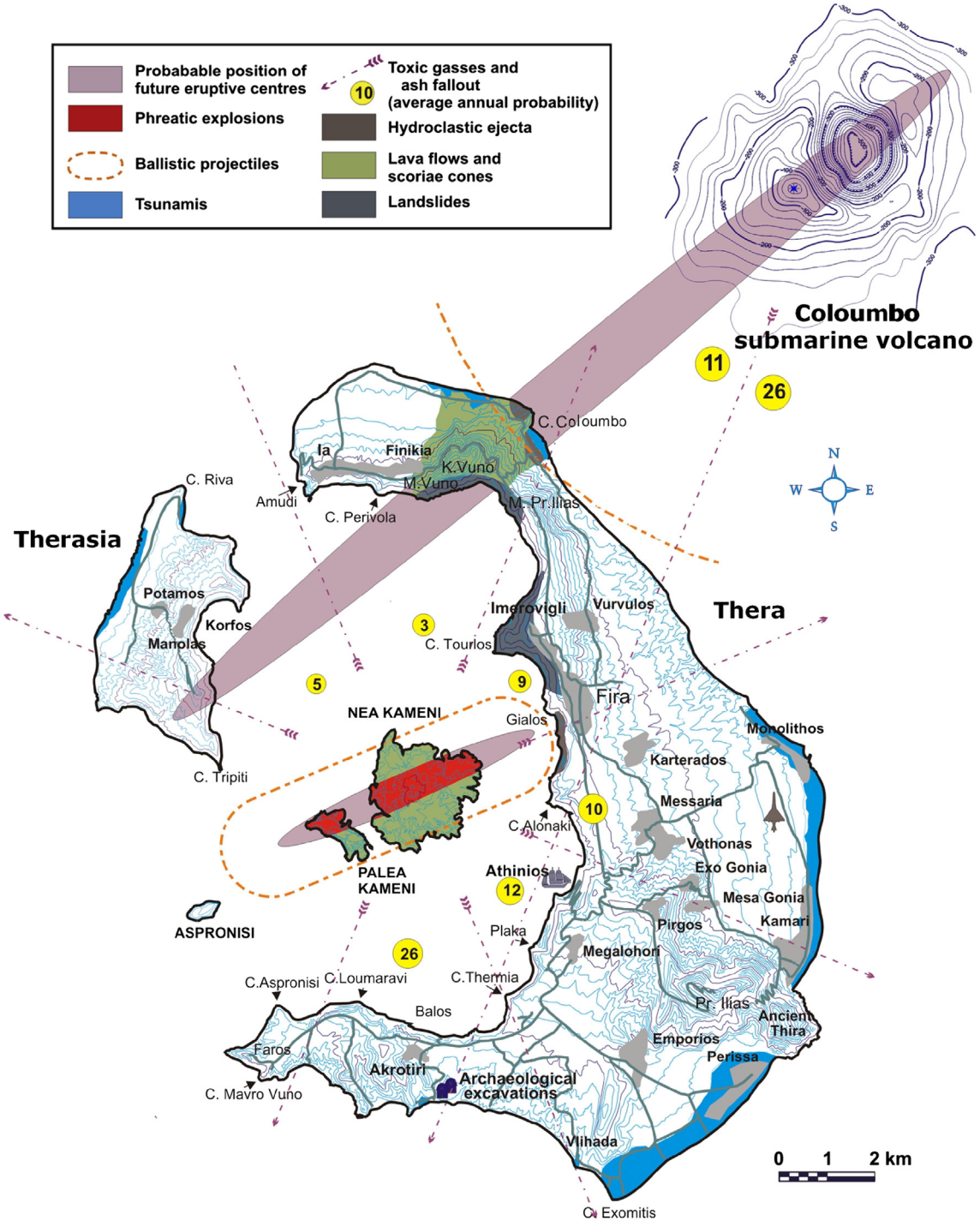

Fig. 1. Map of the Santorini island complex also depicting the volcanic hazards zonation due to a future eruption within the caldera or at Coloumbo submarine volcano. Contours show the bathymetry in meters around the Coloumbo crater. The map has been published by Vougioukalakis and Fytikas (2005) and is also available from http://ismosav.santorini.net website.

VBPs under the influence of gravity and drag forces assuming that air density in the atmosphere varies only with altitude. Finally, the results obtained from all these simulations and their implications for the hazard zonation on Thera are analyzed and discussed.

2. Methods

2.1. Ballistic model

The two forces that act on VBPs and greatly influence their trajectories are namely the drag against the atmospheric air and the gravitational attraction of the Earth. By using Newton's second law of motion and considering the acceleration of a VBP in the horizontal (x) and vertical (z) direction, it is possible to obtain the following system of ordinary differential equations (Alatorre-Ibargüengoitia et al., 2012)

$$\frac{dv_x}{dt} = -\frac{AC_d\rho_a(z)(v_x-u_x)|v-u|}{2m} \quad (1)$$

$$\frac{dv_z}{dt} = -\frac{AC_d\rho_a(z)v_z|v-u|}{2m} - g \quad (2)$$

where v_x and v_z are the horizontal and vertical velocity of the VBP and $\mathbf{v} = (v_x, v_z)$ is its velocity vector, t is time, A and m are the cross-sectional area and mass of the VBP respectively, C_d is the drag-coefficient, $\rho_a(z)$ is air density as a function of altitude z, $\mathbf{u} = (u_x, 0)$ is wind velocity, g is the acceleration of gravity and the quantity $|v - u|$ is given by

$$|v-u| = \sqrt{(v_x-u_x)^2 + v_z^2}. \quad (3)$$

The ratio A/m can be substituted by the quantity $3/(2\rho_b D)$ where ρ_b is the density of VBP and D its diameter (average length of three perpendicular dimensions), provided that the shape of the VBP can be approximated as ellipsoidal. The ejection angle θ also significantly influences the final horizontal range of VBPs by controlling the absolute values of the two velocity components ($v \cos\theta$, $v \sin\theta$) (Fig. 2).

The air density changes with elevation and therefore needs to be recalculated at each point in the trajectory of the VBP. This is done by considering air as a perfect gas, in which case the pressure p at a given elevation z can be calculated following a procedure similar to the one used by Mastin (2001) with

$$p = p_0\left(1-\frac{Lz}{T_0}\right)^{\frac{gM_m}{RL}} \quad (4)$$

where p_0 and T_0 are the pressure (in Pa) and temperature (in K) at sea level, R is the ideal gas constant, M_m is molar mass of dry air and L is the thermal lapse rate. The air density will then be calculated as $\rho_a(z) = pM_m/RT$ and Table 1 gives the numerical values used throughout this study for air density calculations.

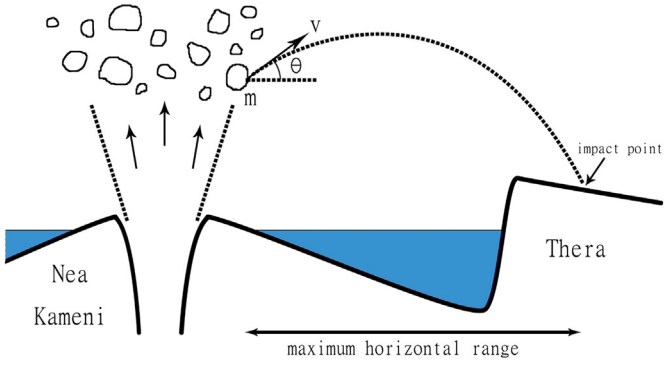

Fig. 2. Cartoon illustrating the physical parameters of a VBP with mass m that is ejected from an eruptive vent in Nea Kameni with a velocity V at an angle θ. The VBP follows a nearly parabolic trajectory before reaching its maximum horizontal range and impacting the Earth's surface in Thera.

The drag coefficient C_d is defined as the dimensionless quantity equal to the drag force divided by the product of kinetic energy and cross-sectional area of the VBP. Obviously the value of C_d greatly depends on the shape of the VBP and its orientation with respect to the flow of air surrounding it. Experimental determinations of drag coefficient for different block shapes (sphere or cube), orientations (side or edge of the cube facing the flow) and variable flow conditions are available (see original work by Hoerner, 1965 later reproduced by Alatorre-Ibargüengoitia and Delgado-Granados, 2006 as well as Maeno et al., 2013). The most important flow parameter that affects the value of the drag coefficient is the Mach number M, where C_d exhibits abrupt changes near $M = 1.0$ while after $M = 3$ the drag coefficient remains almost constant (Fig. 3). The approach adopted here is that at each calculation step the Mach number is calculated as v/c, where v is the velocity of VBP and c is the sound speed in air ($= \sqrt{\gamma RT}$), and then the appropriate C_d is used for solving the ballistic model equations. The drag coefficient is also dependent on the Reynolds number of the flow, however, except from the simple case of a sphere, for any other VBP shape this dependence is quite complicated and it is not included in the following simulations.

In the early 1990s Fagents and Wilson (1993) questioned the assumption used by previous studies that VBPs are ejected into still air and argued that after exiting the vent, VBPs are rather enveloped in a cloud of expanding gas, tephra and other fragments that move roughly at the same velocity. This has the important consequence that under such conditions drag is reduced for the VBPs at least up to some distance from the erupting vent. One way to include such a reduced drag zone in the ballistic model is by considering that the drag coefficient C_d is varying as a function of radial distance r from the erupting vent (Mastin, 2001)

$$C_{dr} = C_d\left(\frac{r}{r_d}\right)^2 \quad (5)$$

where C_{dr} is the new reduced drag coefficient and r_d is the extent of the reduced drag zone. The choice of r_d is rather arbitrary and in subsequent calculations several values are assumed and the effect of this parameter on the VBP horizontal range is explored empirically. After including all these effects and solving the ballistic model equations, the maximum horizontal range of a VBP is defined as the horizontal range x from the ejection point to the point of impact considering also the topographic conditions.

2.2. Calculation of initial velocities

2.2.1. Initial velocities for small VEI eruptions

A suitable value for the initial conditions (position, velocity) of the VBP at the eruptive vent has to be known in order to initiate the solution of the ballistic model equations. These initial conditions are inherently related to the eruption style which in turn depends on parameters such as pressure inside the vent and gas content. According to one definition (Alatorre-Ibargüengoitia et al., 2010) vulcanian eruptions are

Table 1
Values used for the calculation of air density as a function of elevation.

Quantity	Value
p_0	10^5 Pa
T_0	288 K
g	9.81 m/s^2
M_m	0.028964 kg/mol
L	0.0065 K/m
R	8.314 J/(mol K)

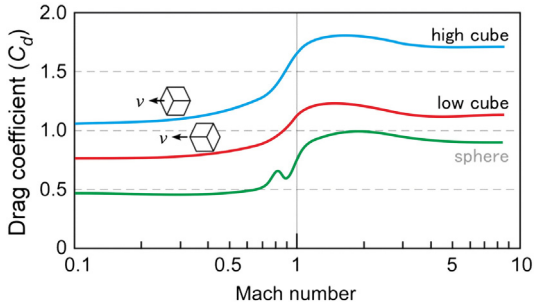

Fig. 3. Diagram showing the variation of the drag coefficient C_d as a function of the Mach number that characterizes the flow regime around the VBP. Three curves are plotted that represent experimentally determined drag coefficients for objects with different shapes (sphere or cube) and orientation (cube facing the flow with its edge, or its side). This diagram is adopted from Maeno et al. (2013) and is based on original data from Hoerner (1965). The figure is published with permission from SpringerOpen.

understood to occur when viscous magma extrudes and solidifies forming a caprock that plugs the eruptive vent. This plug can then be broken up after a short-lived explosion and, as shown by Gottsmann et al. (2011), this switching from effusive to explosive activity may come with very little warning. The destruction of the caprock may produce numerous VBPs, therefore using such an eruption scenario is quite relevant in the effort to calculate initial conditions for the ballistic model. Alatorre-Ibargüengoitia et al. (2010) suggested a model for vulcanian eruptions that takes into account the energy balance during rapid decompression of pressurized magma below a caprock, followed by fragmentation and acceleration of particles. This model has been validated in the laboratory through decompression experiments at different temperature and initial pressures. Furthermore, fragments are assumed to behave as a coherent plug retaining the original cross-sectional area with no escape of the expanding gas at least during the first few seconds of the acceleration phase. Fragmentation is expected to consume a significant amount of energy, therefore the effective pressure P_{ef} available for particle ejection is

$$P_{ef} = P_0 - P_{th} \tag{6}$$

where P_0 is the initial gas pressure and P_{th} is the fragmentation threshold of the magma defined by Spieler et al. (2004) as the minimum pressure differential that can completely fragment the pressurized porous magma. The ordinary differential equation that describes the motion of the caprock propelled by the expansion of a gas–particle mixture is (Alatorre-Ibargüengoitia et al., 2010)

$$\frac{dv_{in}}{dt} = \frac{A}{m_c}\left\{P_{ef}\left[1-\frac{1}{2}(\gamma-1)\frac{v_{in}}{\sqrt{n\gamma R_g T_0}}\right]^{\frac{2\gamma}{\gamma-1}} - P_{ext}\right\} - g \tag{7}$$

where v_{in} is initial velocity, m_c and A_c are mass and cross-sectional area of the caprock, γ is the specific heat capacity ratio of the mixture considering only the fraction of particles in thermal equilibrium with gas, n is the mass fraction of gas, R_g is the gas constant, T_0 is initial temperature and P_{ext} is pressure above the caprock. It should be noted that the ratio A_c/m_c can be substituted by the product $\rho_b H$ where ρ_b is density of the caprock and H its thickness.

An important model parameter that has to be defined is that of the effective pressure available for VBP ejection, which in turn depends on the value of the initial pressure within the conduit and the fragmentation threshold of the magma. The latter quantity is taken equal to 2 MPa, a value that has been experimentally estimated by Spieler et al. (2004) for dacite samples from Santorini. An estimate of the initial pressure below the caprock is more difficult to make, as it depends on which physical process is dominant in generating overpressure within the conduit. Burgisser et al. (2011) identified four such processes namely gas accumulation, conduit wall elasticity, microlite crystallization and magma flow. Theoretical calculations reveal that wall elasticity and microlite crystallization are associated with overpressure values less than 10 MPa, while gas accumulation and magma flow can induce overpressure levels of up to 32 MPa. The authors finally conclude that the latter two processes are more likely to contribute towards high initial pressures within the conduit resulting in explosive behavior. As the purpose of this study is to calculate maximum horizontal ranges of VBPs, an initial pressure of 25 MPa is adopted which implies an overpressure towards the upper end of the range calculated by Burgisser et al. (2011). This value is also higher than the initial pressure estimated for Popocatépetl volcano (11–13 MPa) and slightly higher than the one estimated for Colima volcano (19–22 MPa) (Alatorre-Ibargüengoitia et al., 2010).

The thickness of the caprock is assumed to be 25 m, however, thickness values down to 9 m do not alter the calculated initial velocities significantly. In the absence of published estimates of density for VBP samples from Santorini, a value of 2300 kg/m^3 consistent with the average density of VBPs found at other volcanoes (e.g., Kilgour et al., 2010; Maeno et al., 2013) is assumed. The pressure above the caprock (P_{ext}) is taken as atmospheric ($\sim 10^5$ Pa), while the gas phase is considered to be composed of water vapor ($\gamma = 1.27$, $R_g = 462$) at a temperature T_0 of 1123 K. The mass fraction of gas over solid components is treated as a free parameter in the range of 0.01–0.08 in order to account not only for the water exsolved from magma, but also for the possible involvement of seawater. Using the values of all these parameters the ordinary differential equation can be solved using an implicit Runge–Kutta method (Hairer and Wanner, 2010) and solutions are obtained for a time range of 0–3 s, which is about the period in which the caprock can be considered as one coherent block before disintegrating. After the vulcanian explosion and before it disintegrates, the caprock reaches a height of 0.9–2.3 km (the higher value being reached at higher gas fraction). Fig. 4 shows how the ejection velocity of VBPs, obtained from the solutions of the caprock model, varies as a function of the gas fraction assumed. It can be seen that for gas mass fractions lower than about 0.02 initial velocities are subsonic ($M < 1$) in contrast to higher values ($n = 0.03$–0.06) where the velocities become supersonic ($M = 1 - 2$).

2.2.2. Initial velocities for large VEI eruptions

The caprock model that was used previously for estimating initial conditions of VBPs during vulcanian eruptions is not appropriate for their higher energy counterparts (VEI > 3). In this section a methodology is described that allows initial velocities of VBPs to be calculated by considering the conversion of the thermal to kinetic energy for eruptions with larger VEI. The thermal energy during explosive eruptions is partitioned into kinetic energy of the pyroclasts and seismic energy that is released by volcanic earthquakes (Pyle, 1995). As the seismic energy released through earthquakes is a small fraction in the order of

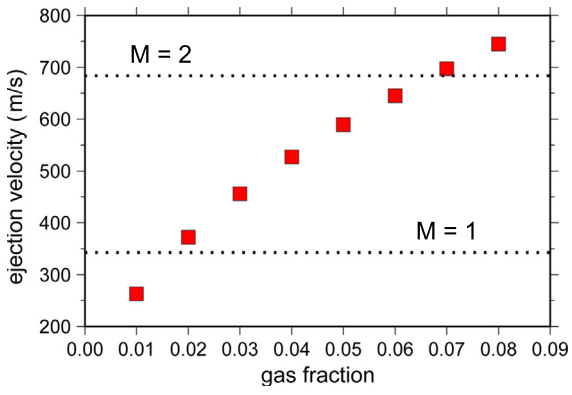

Fig. 4. Diagram showing the variation of ejection velocity of VBPs during vulcanian eruptions using the model of Alatorre-Ibargüengoitia et al. (2010) as a function of the assumed gas mass fraction. The horizontal dotted lines at 340 m/s and 680 m/s represent the Mach number equal to 1 and 2 respectively.

10^{-4} of the kinetic energy (Nairn and Self, 1978), only the conversion of thermal to kinetic energy is of importance. Considering that kinetic energy per unit of time is $\tilde{E}_k$ and thermal energy per unit of time is $\tilde{E}_{th}$, then their relationship is

$$\tilde{E}_k = \eta \tilde{E}_{th} \tag{8}$$

where η is a coefficient that signifies the efficiency of conversion from the one form of energy to the other. If $\tilde{M}$ is the mass released per unit of time it is possible to approximate the velocity at which the material leaves the eruptive vent as

$$v_{in} = \sqrt{\frac{2\eta \tilde{E}_{th}}{\tilde{M}}}. \tag{9}$$

The basic assumption that underlies the methodology presented herein is that all the eruptive processes that contribute to eject VBPs to a maximum horizontal distance are expressed through this conversion of thermal to kinetic energy. Pyle (1995) estimated from first principles thermal energy and mass released per unit of time for explosive eruptions with VEI between 2 and 7 based on the assumption that eruptions with VEI = 2 are primarily basaltic or andesitic and that as the VEI increases eruptions become progressively more silicic. On the other hand, Sato and Taniguchi (1997) have determined conversion efficiency η for a number of magmatic and phreato-magmatic eruptions. The former kind of eruptions has the lowest conversion efficiency (10^{-4}–10^{-2}) in contrast to the latter kind where the mixing of water with magma increases the efficiency coefficient significantly η (~0.01–0.1). This methodology will be applied for calculating initial velocities of larger eruptions originating at Santorini caldera where the possibility of water–magma interaction is likely to lead to increased conversion efficiency, ejecting VBPs at great distances from the erupting vent.

3. Results

3.1. Maximum horizontal range during small eruptions

Initial velocity and corresponding caprock height above the vent were inserted as initial conditions in the ballistic model equations. The VBPs shape is taken as a cube whose corner is orientated at the leading edge ('low-cube'), since this configuration allows a lower drag coefficient resulting in less air resistance and larger horizontal ranges (cf. Fig. 3). Four different sizes of VBPs are assumed (0.35 m, 1.0 m, 2.0 m and 3.0 m) using the same rock density as for the caprock. At this point it should be mentioned that projectiles with sizes smaller than 0.1 m do not follow in general ballistic trajectories, but are rather carried away from the vent by the eruptive column flow (Alatorre-Ibargüengoitia et al., 2012). As the main interest of this study is the maximum horizontal range of VBPs, in all subsequent calculations a tailwind velocity of 20 m/s is assumed. This value corresponds to a wind of grade 8 in the 12-grade Beaufort scale (a grade that is often observed in the Aegean Sea) and can increase the VBPs horizontal range by 15%. In general, visual observations of the extent of the cloud of tephra and fragments where drag is reduced, are in the order of several hundred meters for small explosive eruptions (Nairn and Self, 1978; Mastin, 2001). Three values for the reduced drag zone extent are investigated here, that of 300 m, 500 m and 800 m respectively. The choice of these particular values lies in the fact that they represent diameters of eruptive vents mapped on the Kameni islands by Pyle and Elliott (2006). The ejection angle θ was varied between 10° and 70° for the purpose of finding its optimum value that maximizes horizontal range. The ballistic model equations are then numerically integrated using again an implicit Runge–Kutta method for each set of initial conditions and corresponding gas fraction, for each VBP diameter and reduced drag zone.

The results corresponding to optimal ejection angles of 40°–50° are summarized in Fig. 5 for each VBP diameter and reduced drag zone, as a function of the gas fraction that was used for estimating initial velocities and distance. It can be readily seen that for a reduced drag zone of 300 m it is the combination of smallest VBP size (0.35 m) and highest gas fraction that results in the maximum horizontal distance from the vent (~2.6 km), while all the other diameters reach distances smaller than 1.7 km. For a reduced drag zone of 500 m a separation of diameters starts to occur with the larger ones (2–3 m) reaching larger horizontal distances due to the increased acceleration they attain and their larger inertia. Finally, when the reduced drag zone becomes 800 m the separation of different diameters based on the maximum horizontal distance is more pronounced, with VBPs of 0.35 m reaching 1.5 km and VBPs with diameter of 3.0 m reaching a horizontal distance of about 3 km. It can be

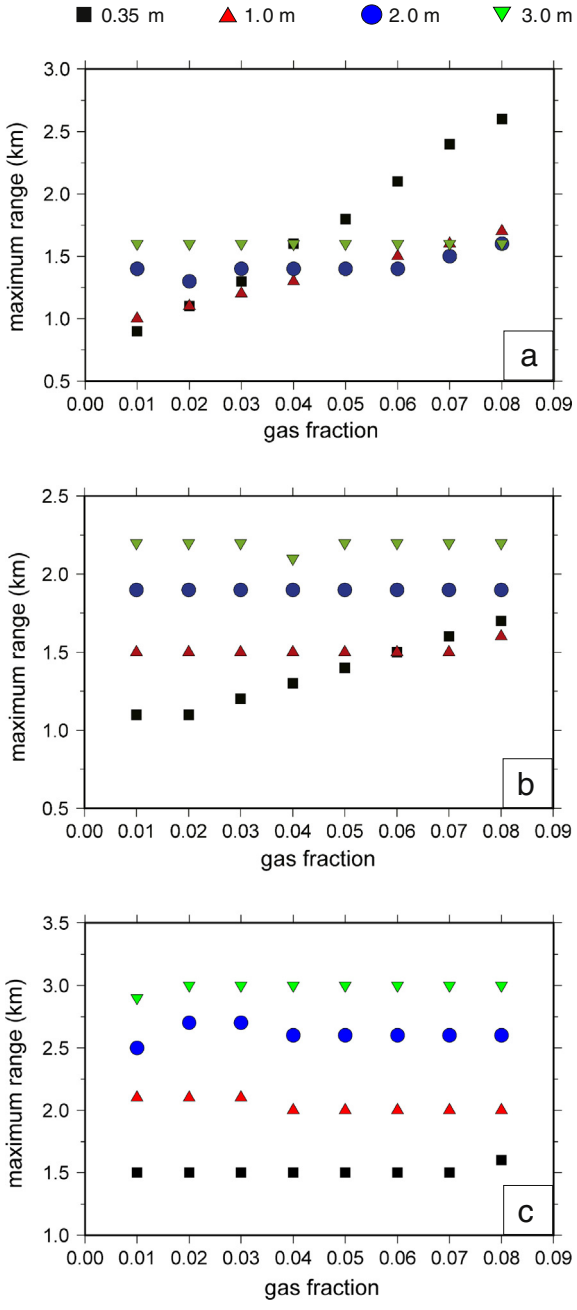

Fig. 5. Summary of the maximum horizontal range obtained for VBPs of different diameters ejected during explosive eruptions consistent with the model of Alatorre-Ibargüengoitia et al. (2010) for reduced drag zone with an extent of (a) 300 m, (b) 500 m and (c) 800 m (see text for more details).

concluded that high gas mass fractions seem to have a strong effect on the maximum horizontal distance only when VBPs have a rather small diameter (<1.0 m). In all other cases it is the extent of the reduced drag zone r_d that seems to significantly affect the maximum horizontal range for larger diameter VBPs.

In order to transform these results into useful information for risk mitigation purposes, maps have to be constructed that will delineate the maximum horizontal ranges after assuming a location for the eruptive vent. Pyle and Elliott (2006) have pointed out that past vent locations exhibit a clear NE-SW trend as a result of the dominant NW-SE direction of extension within the Santorini caldera. They also argue that in all likelihood a future eruption may originate anywhere along this line (also referred to as 'Kameni line' in the literature). Based on this argument two potential vent locations are chosen, one in the Palea and the other on the NE part of Nea Kameni, both of them lying above sea level. A third vent location along the Kameni line is chosen in the area between Nea Kameni and Thera. Due to the proximity of this location to Thera, it is important to consider whether the development of a submarine vent there is possible or not. Recently, Watts et al. (2015) published detailed bathymetric maps of the intra-caldera area which were compared to historic bathymetric charts of the British Admiralty, for the purpose of finding changes in the seafloor due to volcanic activity. This comparison revealed the progressive enlargement of Nea Kameni since 1848 and the shallowing of the seafloor at its NE part as more erupted lava was accumulated there. A shoal reaching to a depth of 35 m below the sea surface, interpreted as old lava flows, was imaged at the location of the potential vent. Pyle and Elliott (2006) also highlight this location as a possible site of a future eruption that will initially start as submarine, but may become subaerial within a few days owing to the high growth rate that lava domes exhibit in Santorini. One could argue that for such a vent location the steep caldera walls (average height 200 m) would act as a natural barrier to any ejected VBPs. However, simple calculations show that for this scenario to happen the vent location must be 238 m away from the caldera walls if the optimum ejection angle is taken as 40° (less than 238 m for larger angles).

Fig. 6 shows the location of the potential vents along with the minimum and maximum horizontal range of different diameter VBPs as suggested by the numerical simulations. These maps reveal that the exact location of the vent in a future eruption will be of crucial importance as to whether populated areas on Thera island will be within the range of VBPs during explosive activity. A vent location on Palea Kameni seems to be the least hazardous for all assumed VBP diameters. On the other hand, the maximum horizontal range of VBPs ejected from a vent located at the submarine shoal covers an area of 1–2 km width along the coast of Thera from Imerovigli to Athinios port. By comparison

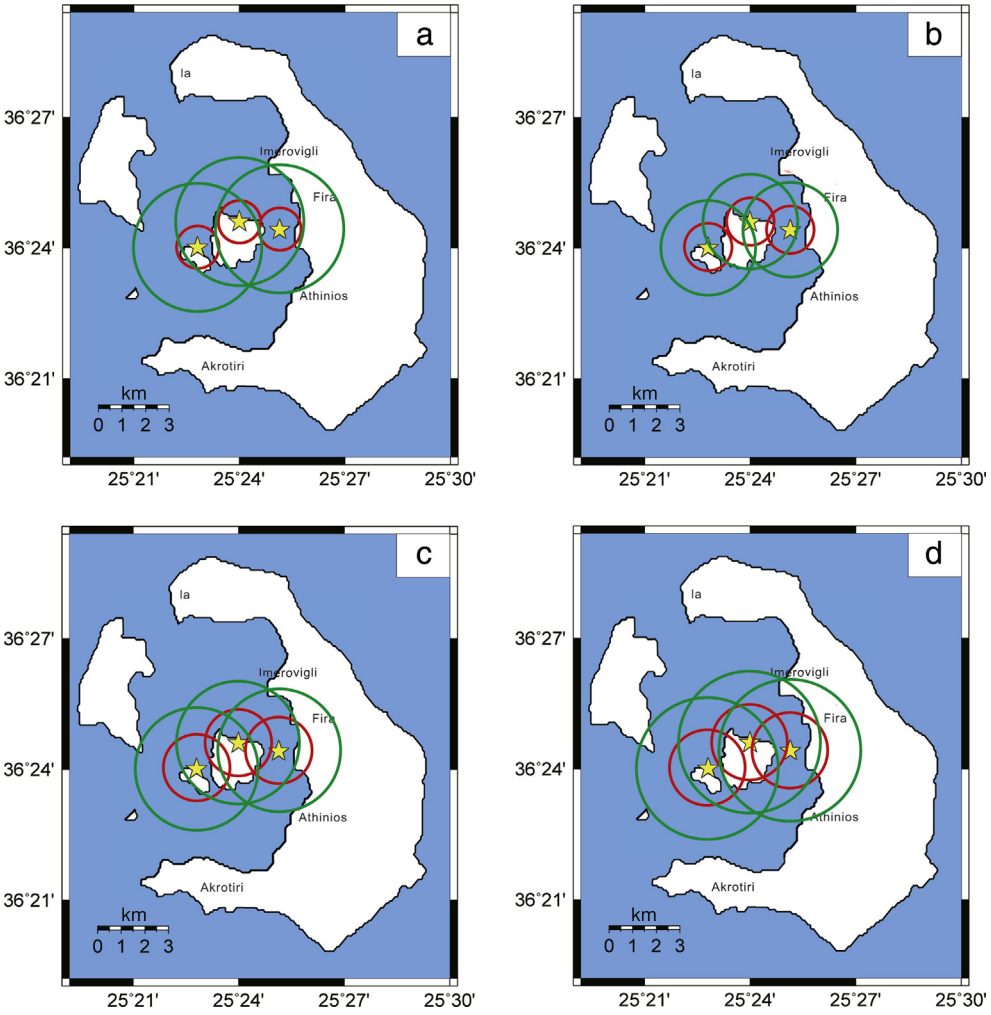

Fig. 6. Maps showing the horizontal range of VBPs ejected during vulcanian-style eruptions for a diameter of (a) 0.35 m, (b) 1.0 m, (c) 2.0 m and (d) 3.0 m. The yellow stars indicate the locations of potential vents along the Kameni line that may develop during a future eruption. The red and green circles represent the minimum and maximum horizontal ranges, respectively, of VBPs launched at optimum angles, but varying initial velocities and zones of reduced drag as shown in Fig. 5. (For interpretation of the references to color in this figure legend, the reader is referred to the web version of this article.)

the VBP hazard zone in Fig. 1 delineated from historical accounts of previous eruptions, is closer to the minimum ranges that VBPs attain in the simulations.

3.2. Maximum horizontal range during large eruptions

Before simulating VBP trajectories for a large eruption, it is necessary to test the validity of the methodology (described in Section 2.2.2) for calculating initial velocities, by trying to model observed VBP horizontal ranges ejected during such an eruption. The Minoan eruption may be a good candidate for such a test, as there is a detailed field survey that identified VBPs ejected during its phreato-magmatic phases and also deciphered their diameters and distribution around the caldera (Pfeiffer, 2001). Field evidence suggests that the Minoan eruption had three phases: in phase 1 the eruptive vents developed and the ejected pumice fell around the caldera, during phase 2 seawater came into contact with magma creating a base surge and finally in phase 3 pyroclastic flows started occurring (Friedrich, 2013). It can be seen that VBPs with a size of about 1.5 m had a maximum horizontal distance of 6–7 km during phase 2 and during phase 3 VBPs with a size of 3.0 m were ejected to a distance of 3–3.5 km around the northern part of the caldera (Fig. 7). It is worth mentioning that Pfeiffer (2001) attempted to model the VBP trajectories, however, his effort was hindered by lack of knowledge of initial velocities as well as his assumption that VBPs were launched into still air (i.e., no reduced drag zone was considered).

The Minoan eruption had a VEI equal to 7 and this value corresponds to thermal energy per unit of time of 10×10^9 W, while the mass flux is 9.5×10^3 kg/s (Pyle, 1995). If the coefficient η is considered to be in the range of 0.01–0.1 the initial velocities calculated from these values range between 145 and 458 m/s. The ballistic equations are first solved using these initial velocities for VBPs with size of 1.5 m, then for a size of 3.0 m and by treating the reduced drag zone as a free parameter which can vary between 1 and 5 km. The vent location is taken to be at sea level as inferred by Pfeiffer (2001) for phases 2–3. The results of these simulations show that the observed horizontal VBP distances during phase 2 can be obtained if $\eta = 0.1$ ($v_{in} = 458$ m/s) and the reduced drag zone has an extent of 2.5–3.5 km (Fig. 8). On the other hand, the observed VBP distances during phase 3 can be achieved with a conversion coefficient equal to 0.02 ($v_{in} = 205$ m/s) and a reduced drag zone ranging from 1 km to 2.5 km. As in the case of smaller eruptions, the optimum ejection angle that is consistent with the observed ranges is between 40° and 50°. Any other combination of these parameters either over- or under-estimates the observed VBP range. These estimates are in accordance with the fact that the activity during phase 2 was phreato-magmatic and therefore a higher conversion efficiency of thermal to kinetic energy should be expected, compared to phase 3 where water involvement was less significant. Additionally, the inferred extent of the reduced drag zone in each phase does not exceed the upper length (~4 km) of the erupting fissure that Pfeiffer's observations suggest.

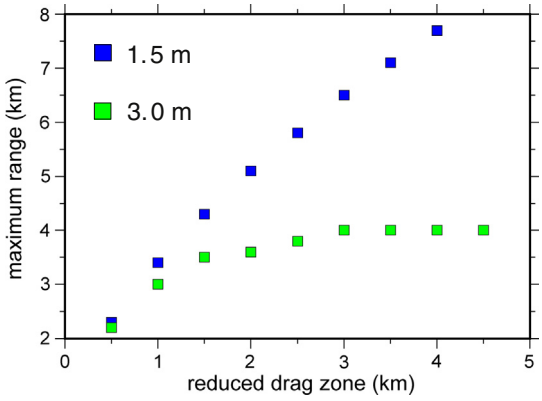

Fig. 8. Variation of maximum horizontal range as a function of the reduced drag zone extent for VBPs during phase 2 (diameter 1.5 m) and phase 3 (diameter 3.0 m) of the Minoan eruption.

Repetition of a Minoan-style eruption in Santorini in the foreseeable future is of course highly unlikely, as an eruption of this magnitude occurs in cycles of about 20 ka (Vougioukalakis and Fytikas, 2005). A more likely scenario however, is that of a phreato-magmatic eruption with VEI equal to 4 which is of similar magnitude to a post-Minoan eruption that occurred within the caldera on July 15, 726 AD. The next step is to simulate VBP trajectories as well as find their maximum horizontal range for such an eruption. Based on the results of Pyle (1995), for VEI = 4 eruption $\tilde{M} = 4.7 \times 10^3$ kg/s and $\tilde{E}_{th} = 5.9 \times 10^9$ W producing an initial velocity of 501 m/s if the conversion efficiency is assumed as maximum ($\eta = 0.1$). The same VBP diameters are utilized as in the case of the vulcanian eruptions (0.35 m, 1.0 m, 2.0 m, 3.0 m), with a density of 2300 kg/m^3 and optimum ejection angle $\theta = 40°$. The extent of the reduced drag zone is taken as 1.5 km assuming an eruption location centered in the Kameni islands representing a series of vents (Fig. 9). Results show a separation of maximum horizontal distance as a function of VBP size, with VBPs between 0.35 and 1.0 m either falling into the sea or marginally reaching the coast of Thera/Therasia. Larger VBPs (2.0–3.0 m) attain higher acceleration and due to their large inertia are capable of impacting populated areas on Thera, but also Therasia (most settlements on Therasia are located along the eastern part of this island).

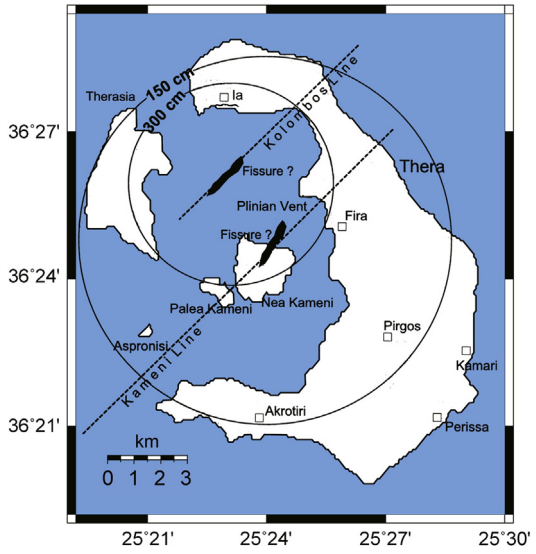

Fig. 7. Map depicting the maximum horizontal range of VBPs from phase 2 (diameter 1.5 m) and 3 (diameter 3 m) during the Minoan eruption. Thick lines across the Kameni and Coloumbo lines represent the suggested fissures where eruptive activity was occurring. The figure is reproduced based on the observations of Pfeiffer (2001).

4. Conclusions

VBPs represent a significant volcanic hazard for the areas around the Santorini caldera owing to the possibility that a future eruption may involve magma and seawater interactions, potentially propelling VBPs at great distances. The simulations performed earlier suggest that VBPs may impact populated areas around the caldera either during a vulcanian-style eruption, or during a higher energy eruption that exhibits maximum conversion efficiency between thermal and kinetic energy. The coastal area from Imerovigli to Athinios port is highlighted by the results of this study as within the range of ejected VBPs during smaller explosive eruptions. In a similar way, a higher energy eruption may eject VBPs to populated areas on Thera (Imerovigli, Fira, Athinios, Akrotiri) and Therasia. Unfortunately, the aforementioned areas include

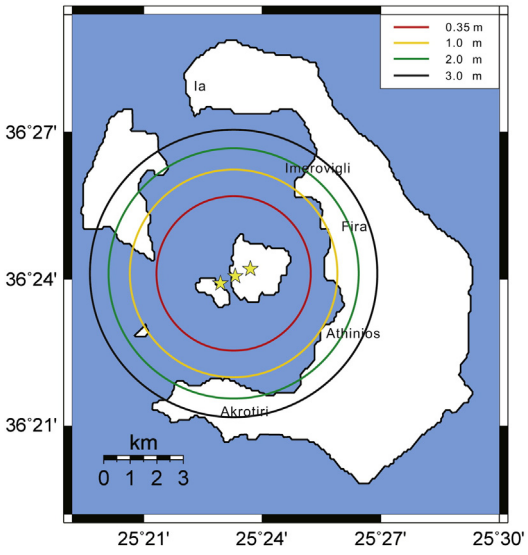

Fig. 9. Map of Santorini islands showing the delineation of the maximum horizontal range for different diameter VBPs (expressed as circles of different color) ejected during an eruption with VEI = 4. The yellow stars across the Kameni islands represent multiple eruptive vents that define a length of approximately 1.5 km equal to the assumed extent of reduced drag zone. (For interpretation of the references to color in this figure legend, the reader is referred to the web version of this article.)

numerous man-made constructions (such as hotels, restaurants, open-air swimming pools) and are favorite places of stay for tens of thousands of visitors every year. Also, a large part of the intra-caldera area could be restricted for ships, placing constraints on the maritime communication of Santorini with the outside world. The results presented here can therefore serve as a general guide for civil protection authorities in order to decide evacuation routes and to establish safety zones for the population as part of their response to VBP hazards during a future eruption. The greatest uncertainty influencing these results obviously has to do with the exact location of the eruptive vent(s) along the Kameni line. In this respect, continuous seismic and geodetic monitoring of the Santorini caldera may give enough a priori clues as to where the eruptive vent may develop, assisting the authorities to adjust their planning accordingly.

It is also important to highlight the limitations that this study entails with respect to the parameters used in the numerical simulations. One such limitation concerns values corresponding to the extent of the reduced drag zone, that have been chosen mostly based on empirical criteria (namely observations from other volcanoes and the vent diameters found on the Kameni islands). More accurate estimates could be obtained by performing modeling of the multiphase carrier flow using a methodology similar to that of de' Michieli Vitturi et al. (2010). Another limitation has to do with VBP densities as well as drag coefficients that could be estimated directly from VBP samples from Santorini rather than assuming an average density and drag coefficients for ideal geometrical shapes like cubes. The presented simulations also did not consider the possibility of collisions between VBPs that may drastically increase their horizontal range up to twice the expected value (Vanderkluysen et al., 2012). It is therefore clear that there is a need for more quantitative studies concerning the impact of volcanic hazards on Santorini that would lead to an improved understanding of the risks posed to the local population as well as the visitors of these islands.

Acknowledgments

I would like to thank the Ministry of Science and Technology, Taiwan for the financial support of this study and the Editor-in-Chief Prof. Lionel Wilson for handling the paper. Thorough and constructive reviews by an anonymous reviewer and Loÿc Vandercluysen substantially improved the quality as well as the clarity of the original manuscript.

References

Alatorre-Ibargüengoitia, M.A., Delgado-Granados, H., 2006. Experimental determination of drag coefficient for volcanic materials: calibration and application of a model to Popocatépetl volcano (Mexico) ballistic projectiles. Geophys. Res. Lett. 33, L11302. http://dx.doi.org/10.1029/2006GL026195.

Alatorre-Ibargüengoitia, M.A., Scheu, B., Dingwell, D.B., Delgado-Granados, H., Taddeucci, J., 2010. Energy consumption by magmatic fragmentation and pyroclast ejection during vulcanian eruptions. Earth Planet. Sci. Lett. 291, 60–69. http://dx.doi.org/10.1016/j.epsl.2009.12.051.

Alatorre-Ibargüengoitia, M.A., Delgado-Granados, H., Dingwell, D.B., 2012. Hazard map for volcanic ballistic impacts at Popocatépetl volcano (Mexico). Bull. Volcanol. 74, 2155–2169. http://dx.doi.org/10.1007/s00445-012-0657-2.

Bond, A., Sparks, R.S.J., 1976. The Minoan eruption of Santorini, Greece. J. Geol. Soc. Lond. 132, 1–16.

Bower, S.M., Woods, A.W., 1996. On the dispersal of clasts from volcanic craters during small explosive eruptions. J. Volcanol. Geotherm. Res. 73, 19–32.

Burgisser, A., Arbaret, L., Druitt, T.H., Giachetti, T., 2011. Pre-explosive conduit conditions of the 1997 vulcanian explosions at Soufriére Hills volcano, Montserrat: II. Overpressure and depth distribution. J. Volcanol. Geotherm. Res. 199, 193–205. http://dx.doi.org/10.1016/j.jvolgeores.2010.11.14.

de' Michieli Vitturi, M., Neri, A., Ongaro, T.E., Lo Savio, S., Boschi, E., 2010. Lagrangian modeling of large volcanic particles: applications to vulcanian explosions. J. Geophys. Res. 115, B08206. http://dx.doi.org/10.1029/2009JB007111.

Dimitriadis, I., Karagianni, E., Panagiotopoulos, D., Papazachos, C., Hatzidimitriou, P., Bohnhoff, M., Rische, M., Meier, T., 2009. Seismicity and active tectonics at Coloumbo Reef (Aegean sea, Greece): monitoring an active volcano at Santorini volcanic center using a temporary seismic network. Tectonophysics 465, 136–149. http://dx.doi.org/10.1016/j.tecto.2008.11.005.

Druitt, T.H., Francaviglia, V., 1992. Caldera formation on Santorini and the physiography of the islands in the late bronze age. Bull. Volcanol. 54, 484–493.

Fagents, S.A., Wilson, L., 1993. Explosive volcanic eruptions — VII. The ranges of pyroclasts ejected in transient volcanic explosions. Geophys. J. Int. 113, 359–370.

Foumelis, M., Trasatti, E., Papageorgiou, E., Stramondo, S., Parcharidis, I., 2013. Monitoring Santorini volcano (Greece) breathing from space. Geophys. J. Int. 193, 161–170. http://dx.doi.org/10.1093/gji/ggs135.

Friedrich, W.L., 2013. The Minoan eruption of Santorini around 1613 BC and its consequences. Tagungen Landesmus. Vorgesch. Halle 9, 37–48.

Gottsmann, J., De Angelis, S., Fournier, N., Van Camp, M., Sacks, S., Linde, A., Ripepe, M., 2011. On the geophysical fingerprint of Vulcanian explosions. Earth Planet. Sci. Lett. 306, 98–104. http://dx.doi.org/10.1016/j.epsl.2011.03.035.

Hairer, E., Wanner, G., 2010. Solving Ordinary Differential Equations II: Stiff and Differential Algebraic Problems. Springer.

Harris, A.J.L., Ripepe, M., Hughes, E.A., 2012. Detailed analysis of particle velocities, size distributions and gas densities during normal explosions at Stromboli. J. Volcanol. Geotherm. Res. 231–232, 109–131. http://dx.doi.org/10.1016/j.jvolgeores.2012.02.012.

Heiken, G., McCoy, F., 1984. Caldera development during the Minoan eruption, Thira, Cyclades, Greece. J. Geophys. Res. 89, 8441–8462.

Hoerner, S.F., 1965. Fluid Dynamic Drag. S. F. Hoerner, New York (450 pp.).

Kilgour, G., Manville, V., Della Pasqua, F., Graettinger, A., Hodgson, K.A., Jolly, G.E., 2010. The 25 September 2007 eruption of Mount Ruapehu, New Zealand: directed ballistics, surtseyan jets, and ice-slurry lahars. J. Volcanol. Geotherm. Res. 191, 1–14. http://dx.doi.org/10.1016/j.jvolgeores.2009.10.015.

Konstantinou, K.I., Evangelidis, C.P., Liang, W.-T., Melis, N.S., Kalogeras, I., 2013. Seismicity, V_p/V_s and shear wave anisotropy variations during the 2011 unrest at Santorini caldera, southern Aegean. J. Volcanol. Geotherm. Res. 267, 57–67. http://dx.doi.org/10.1016/j.jvolgeores.2013.10.001.

Lagios, E., Sakkas, V., Novali, F., Bellotti, F., Ferretti, A., Vlachou, K., Dietrich, V., 2013. SqeeSAR and GPS ground deformation monitoring of Santorini Volcano (1992–2012): tectonic implications. Tectonophysics 594, 38–59. http://dx.doi.org/10.11016/j.tecto.2013.03.012.

Maeno, F., Nakada, S., Nagai, M., Kozono, T., 2013. Ballistic ejecta and eruption condition of the vulcanian explosion of Shinmoedake volcano, Kyushu, Japan on 1 February 2011. Earth Planets Space 65, 609–621. http://dx.doi.org/10.5047/eps.2013.03.004.

Mastin, L.G., 2001. A simple Calculator of Ballistic Trajectories for Blocks Ejected During Volcanic Eruptions. US Geological Survey, Open-File report 01–45.

Nairn, I.A., Self, S., 1978. Explosive eruptions and pyroclastic avalanches from Ngauruhoe in February 1975. J. Volcanol. Geotherm. Res. 3, 39–60.

Newhall, C.G., Self, S., 1982. The Volcanic Explosivity Index (VEI) an estimate of explosive magnitude for historical volcanism. J. Geophys. Res. 87, 1231–1238.

Newman, A.V., Stiros, S., Feng, L., Psimoulis, P., Moschas, F., Saltogianni, V., Jiang, Y., Papazachos, C., Panagiotopoulos, D., Karagianni, E., Vamvakaris, D., 2012. Recent geodetic unrest at Santorini caldera, Greece. Geophys. Res. Lett. 39, L06309. http://dx.doi.org/10.1029/2012GL051286.

Papoutsis, I., Papanikolaou, X., Floyd, M., Ji, K.H., Kontoes, C., Paradissis, D., Zacharis, V., 2013. Mapping inflation at Santorini volcano, Greece, using GPS and InSAR. Geophys. Res. Lett. 40. http://dx.doi.org/10.1029/2012GL054137.

Parks, M.M., Biggs, J., England, P., Mather, T.A., Nomikou, P., Palamartchouk, K., Papanikolaou, X., Paradissis, D., Parsons, B., Pyle, D.M., Raptakis, C., Zacharis, V., 2012. Evolution of Santorini volcano dominated by episodic and rapid fluxes of melt from depth. Nat. Geosci. 1–6 http://dx.doi.org/10.1038/ngeo1562.

Pfeiffer, T., 2001. Vent development during the Minoan eruption (1640 BC) of Santorini, Greece, as suggested by ballistic blocks. J. Volcanol. Geotherm. Res. 106, 229–242.
Pyle, D.M., 1995. Mass and energy budgets of explosive volcanic eruptions. Geophys. Res. Lett. 22, 563–566.
Pyle, D.M., Elliott, J.R., 2006. Quantitative morphology, recent evolution and future activity of the Kameni Islands volcano, Santorini, Greece. Geosphere 2, 253–268. http://dx.doi.org/10.1130/GES00028.1.
Sato, H., Taniguchi, H., 1997. Relationship between crater size and ejecta volume of recent magmatic and phreato-magmatic eruptions: implications for energy partitioning. Geophys. Res. Lett. 24, 205–208.
Spieler, O., Kennedy, B., Kueppers, U., Dingwell, D.B., Scheu, B., Taddeucci, J., 2004. The fragmentation threshold of pyroclastic rocks. Earth Planet. Sci. Lett. 226, 139–148. http://dx.doi.org/10.1016/j.epsl.2004.07.016.
Vanderkluysen, L., Harris, A.J.L., Kelfoun, K., Bonadonna, C., Ripepe, M., 2012. Bombs behaving badly: unexpected trajectories and cooling of volcanic projectiles. Bull. Volcanol. 74, 1849–1858. http://dx.doi.org/10.1007/s00445-012-0635-8.
Vougioukalakis, G.E., Fytikas, M., 2005. Volcanic hazards in the Aegean area, relative risk evaluation, monitoring, and present state of the active volcanic centers, the south Aegean active volcanic arc: present knowledge and future perspectives. Dev. Volcanol. 7, 161–183.
Walker, G.P.L., Wilson, L., Bowell, E.L.G., 1971. Explosive volcanic eruptions — I. The rate of fall of pyroclasts. Geophys. J. R. Astron. Soc. 22, 377–383.
Watts, A.B., Nomikou, P., Moore, J.D.P., Parks, M.M., Alexandri, M., 2015. Historical bathymetric charts and the evolution of the Santorini submarine volcano. Geochem. Geophys. Geosyst. 847–869 http://dx.doi.org/10.1002/2014GC005679.
Wilson, L., 1972. Explosive volcanic eruptions — II. The atmospheric trajectories of pyroclasts. Geophys. J. R. Astron. Soc. 30, 381–392.
Yamagishi, H., Feebrey, C., 1994. Ballistic ejecta from the 1988–1989 andesitic vulcanian eruption of Tokachidake volcano, Japan, — morphological features and genesis. J. Volcanol. Geotherm. Res. 59, 269–278.